Title	Period-doubling cascades of canards from the extended Bonhoeffer–van der Pol oscillator
Author(s)	Sekikawa, Munehisa; Inaba, Naohiko; Yoshinaga, Tetsuya; Hikihara, Takashi
Citation	Physics Letters A (2010), 374(36): 3745-3751
Issue Date	2010-08-09
URL	http://hdl.handle.net/2433/134570
Right	© 2010 Elsevier B.V.
Type	Journal Article
Textversion	author

Period-Doubling Cascades of Canards from the Extended Bonhoeffer-van der Pol Oscillator

Munehisa Sekikawa [a], Naohiko Inaba [b], Tetsuya Yoshinaga [c], and Takashi Hikihara [a]

[a] *Department of Electrical Engineering, Graduate School of Engineering, Kyoto University; Katsura, Nishikyo, Kyoto, 615-8510 Japan*

[b] *Department of Electronics and Bioinformatics, Meiji University; 1-1-1 Higashi-Mita, Tama-ku, Kawasaki, 214-8571 Japan*

[c] *Institute of Health Biosciences, The University of Tokushima; 3-18-15 Kuramoto-cho, Tokushima, 770-8509 Japan*

Abstract

This letter investigates the period-doubling cascades of canards, generated in the extended Bonhoeffer-van der Pol oscillator. Canards appear by Andronov Hopf bifurcations (AHBs) and it is confirmed that these AHBs are always supercritical in our system. The cascades of period-doubling bifurcation are followed by mixed-mode oscillations. The detailed two-parameter bifurcation diagrams are derived, and it is clarified that the period-doubling bifurcations arise from a narrow parameter value range at which the original canard in the non-extended equation is observed.

Key words: Andronov Hopf bifurcations, mixed-mode oscillations, canards, chaos
PACS: 05.45.-a, 05.45.Ac, 05.45.Pq

1 Introduction

In a simple second-order differential equation such as the van der Pol oscillator, in some cases, the amplitude of the limit cycle grows abnormally fast as a control parameter is varied [1–5]. This phenomenon is called a canard [4], because the oscillatory trajectory in phase space resembles a duck. It is also called a lost solution [3], because this solution behaves as if the trajectory has ceased to exist. Canards are observed in slow-fast systems that contain a small parameter ε. It has been shown, using the techniques of non-standard analysis, that the amplitude changes on the order of 1 when the control parameter is varied on the order of $\exp(-1/\varepsilon)$ [4]. $\exp(-1/\varepsilon)$ is approximated by 4.5×10^{-5} if $\varepsilon = 0.1$ and by 3.7×10^{-44} if $\varepsilon = 0.01$. Thus, the amplitude of the limit cycle is extremely sensitive to the control parameter ε. $\varepsilon = 0.1$–0.01 can be easily implemented in laboratory experiments [6,7].

Mixed-mode oscillations (MMOs) have been an area of intense research in recent years [9–15]. They consist of a sequence of alternating period-adding phenomena and chaotically spiking canards [8]. They have been observed numerically and experimentally in many systems, from chemical kinetics [9] to electrical circuits [10–12]. However, there has been little discussion on bifurcation, which fills the gap between the canard in the original second-order equation and the MMOs generated in an extended higher-dimensional equation. Moreover, the influence of variations in the system parameter ε on MMOs has not been discussed in detail.

Email address: sekikawa@dove.kuee.kyoto-u.ac.jp

Present address: Aihara Innovative Mathematical Modelling Project, FIRST, JST; 4-6-1 Komaba, Meguro-ku, Tokyo, 153-8505 Japan. (Munehisa Sekikawa).

Our objective in this letter is to obtain a two-parameter bifurcation diagram of the period-doubling bifurcation of canards, which are the origin of MMOs, as generated by the following extended Bonhoeffervan der Pol (BVP) equation [17,18]:

$$\begin{cases} \varepsilon\dot{x} = x(1-x^2) + y + z \\ \dot{y} \;\; = -x - k_1 y + B_0 \\ \dot{z} \;\; = k_3(-x - k_2 z + B_1), \end{cases} \tag{1}$$

where $0 < \varepsilon \ll 1$ is assumed. If $k_3 = 0$, Eq. (1) is reduced to the BVP equation, which can generate canards. Equation (1) is considered to be a naturally extended third-order model of the BVP equation [16,17]. The extended BVP equation is well known to exhibit chaos [16–18], but the relationship between canards and chaos in this equation has not yet been discussed in detail.

For simplicity, the parameter restrictions $k_1 = k_2$ and $B_0 = B_1$ are assumed; that is,

$$\begin{cases} \varepsilon\dot{x} = x(1-x^2) + y + z \\ \dot{y} \;\; = -x - k_1 y + B_0 \\ \dot{z} \;\; = k_3(-x - k_1 z + B_0). \end{cases} \tag{2}$$

Here, note that there is another way to reduce this to the BVP oscillator. If $k_3 = 1$, $(x, y + z)$ is also equivalent to the BVP equation. We are interested in what happens if the parameter k_3 is varied slightly when k_1 and B_0 are set such that canards are generated by this equation.

Figures 1 (a), (b), and (c) show time evolutions obtained from numerical simulation of Eq. (2). The time evolution in Fig. 1 (a) consists of one large and four small excursions, Fig. 1 (b) consists of one large and three small excursions, and so on. We consider that these phenomena can be called MMOs on the basis of their wave forms.

Some excellent discussions on the MMO mechanism have been reported recently [19–21]. Medvedev and Yoo showed that the generation of MMOs and chaos is explained well if subcritical AndronovHopf bifurcations (AHBs) exist. However, in our case, we have confirmed that the AHBs are always supercritical by calculating a one-parameter bifurcation diagram using the software XPPAUT [22]. The mechanism of the MMOs and chaos observed in our system could differ from that in Medvedev and Yoo's scenario [19,20]. Moreover, our system is not a three-time-scale system [21].

Drawing a bifurcation diagram reveals that period-doubling cascades of canards, which lead to MMOs, exist in a narrow parameter value region where the original canard exists in the non-extended equation.

2 Circuit setup

To discuss the relationship between the canard in a two-dimensional circuit and MMOs in a higher-dimensional circuit, we analyze the extended BVP oscillator, which is illustrated in Fig. 2. In the figure, *N.C.* is a nonlinear conductance. A small capacitance is chosen. We consider the case in which the $v-i$ characteristics of the conductance are represented by the third-order

polynomial function as follows:

$$i_n(v) = -g_1 v + g_3 v^3, \tag{3}$$

where $i_n(v)$ is the current through the conductance, and v is the voltage. Here, v, i_1, and i_2 are the state variables. Then, from Kirchhoff's laws, the governing equation of the circuit is expressed by the third-order autonomous differential equation as follows:

$$\begin{cases} C\dfrac{\mathrm{d}v}{\mathrm{d}t} &= i_1 + i_2 - i_n(v) \\ L_1\dfrac{\mathrm{d}i_1}{\mathrm{d}t} &= -v - r_1 i_1 + E_1 \\ L_2\dfrac{\mathrm{d}i_2}{\mathrm{d}t} &= -v - r_2 i_2 + E_2, \end{cases} \tag{4}$$

where r_1 and r_2 are resistances. By changing each variable and constant as follows:

$$\begin{aligned} v = \sqrt{\frac{g_1}{g_3}}x,\ i_1 = g_1\sqrt{\frac{g_1}{g_3}}y,\ i_3 = g_1\sqrt{\frac{g_1}{g_3}}z, \\ E_1 = \sqrt{\frac{g_1}{g_3}}B_1,\ E_2 = \sqrt{\frac{g_1}{g_3}}B_2,\ \varepsilon = \frac{C}{L_1 g_1^2},\ t = L_1 g_1 \tau, \\ k_1 = g_1 r_1,\ k_2 = g_1 r_2,\ k_3 = \frac{L_1}{L_2},\ `\bullet' = \frac{d}{d\tau}, \end{aligned} \tag{5}$$

Eq. (1), which is a normalized version of Eq. (4), is obtained. k_3 is the ratio of the inductors. Equation (4) is well known to be capable of generating chaos [16]. An example of a chaotic attractor is shown in Fig. 3.

3 Bifurcation structure of the extended BVP oscillator

To discuss the relationship between the canard observed in the BVP oscillator and the MMOs generated in the extended BVP oscillator, this study analyzes Eq. (2), assuming

$$0 < k_3 < 1. \tag{6}$$

At $k_1 = 0.35$ and $k_3 = 1$, a canard is observed around $B_0 \simeq 0.486$, as shown in Fig. 4. The following discussion considers $\varepsilon = 0.09$–0.1. The canard phenomenon is enhanced at smaller ε. However, $\exp(-1/\varepsilon)|_{\varepsilon=0.01} \simeq 10^{-44}$. Since the solution for ε is stressed, it is desirable to choose $\varepsilon = 0.09$–0.1 in the numerical calculations.

Figure 5 presents a bifurcation diagram for $\varepsilon = 0.1$. AHBs occur at $B_0 = \pm 0.5$. The AHBs are explicitly calculated manually. The AHB which occurs when $B_0 = 0.5$ is illustrated in Fig. 5. Period-doubling bifurcations are generated when k_3 is decreased. These period-doubling bifurcation curves are obtained by the shooting algorithm proposed in [23]. In the figure, I^1 is the first period-doubling bifurcation curve, and I^2 is the second. In the upper region of I^1, a periodic orbit with period 1 is generated and in the region between I^1 and I^2, a periodic orbit with period 2 is generated. The accumulation of period-doubling bifurcations is well known as the typical route to chaos.

A previous paper about the mechanism that generates MMOs and chaos [20] asserts that the MMO mechanism is easily explained if subcritical AHBs exist. However, in our case, numerical results using the XPPAUT software indicate that the two AHBs are always supercritical. The one-parameter bifurcation

diagram obtained by XPPAUT is presented in Fig. 6 (a). The magnified diagram in Fig. 6 (b) shows that the AHB is supercritical at $B_0 = 0.5$. This result and the above mentioned discussion indicate that MMOs and chaos can occur in a system that does not include subcritical AHBs.

Figure 7 presents a magnified version of Fig. 5. The bifurcation curves I^1, I^2, I^4, I^8, and I^{16} are drawn in the figure. The largest Liapunov exponent is calculated using the method in [24]; a positive largest Liapunov exponent indicates chaos. Regions where chaos is observed are shaded in the figure. This figure clearly shows that the canards are very sensitive to changes in k_3 and B_0. Note that the period-doubling bifurcation curves have a steep point in the parameter range at which the original canard is observed ($B_0 \simeq 0.49$).

Figures 8 (a) and (b) present a one-parameter bifurcation diagram and the corresponding Liapunov exponents, respectively. A magnified version of the one-parameter bifurcation diagram that shows period-doubling accumulation is presented in Fig. 8 (a2). Here, B_0 is fixed at 0.49, and k_3 is chosen as a bifurcation parameter. The largest Liapunov exponent and the second Liapunov exponent are estimated by the method in [24]. Since the system is autonomous, one of the three Liapunov exponents is always zero. These changes in exponent clearly explain the appearance of period-doubling bifurcation, which is the route to chaos. From a broad view of Fig. 8 (a1), the attractor with period 2 is followed by the attractor with period 3, which is followed by the attractor with period 4. These period-adding transitions are the MMOs (Fig. 1).

Here, we focus on the period-doubling bifurcations. Examples of attractors projected to the $(x,\ y + z)$ plane are presented in Fig. 9. In this figure, (a), (b), (c), and (d) correspond to periodic attractors with periods 1, 2, 4, and 8,

respectively. Figure 10 (a) shows a chaotic attractor consisting of canards with small-, medium-, and large-amplitude oscillations. Unimodality is observed in the works of Medvedev and Yoo [19,20]. We constructed the first return map for a chaotic attractor in a similar manner. Unimodality is also confirmed as shown in Fig. 10 (b).

Next, we show the two-parameter bifurcation diagram in the case of $\varepsilon = 0.09$ (Fig. 11). In the figure, I^1 and I^2 are the period-doubling bifurcation curves, which are steeper than those for $\varepsilon = 0.1$. This tendency is more prominent as far as our numerical results are concerned; we are interested in this tendency. However, we could not draw I^4 because of insufficient computational precision. We could not draw even I^1 in the case of $\varepsilon = 0.085$.

4 Concluding remarks

In this letter, we analyzed the extended BVP oscillator, which generates a period-doubling bifurcation route to chaos and obtained two-parameter bifurcation diagrams. It was confirmed that AHBs in our system were always supercritical and the period-doubling bifurcation curves have a steep point in the parameter value range at which the original canard was observed. In the future, it could be interesting to analyze this model with higher precision and to observe this phenomenon in laboratory experiments.

References

[1] E. Benoit, J. L. Callot, F. Diener, and M. Diener, IRMA, Strasbourg, France, (1980).

[2] M. Diener, *Math. Intelligencer* **6** (1984) 38.

[3] A. K. Zvonkin and M. A. Shubin, *Russian Math. Surveys* **39** (1984) 69.

[4] V. I. Arnol'd (Ed.), Encyclopedia of Mathematical Sciences **5** Springer-Verlag, 1994.

[5] J. Guckenheimer, K. Hoffman, and W. Weckersser, *Int. J. Bifurc. Chaos* **10** (2000) 2669.

[6] M. Itoh and R. Tomiyasu, *IEICE Trans. Fundam. Electron. Commun. Comput. Sci.* **E73** (6) (1990) 848.

[7] M. Itoh and R. Tomiyasu, *IEICE Trans. Fundam. Electron. Commun. Comput. Sci.* **E73** (11) (1990) 1866.

[8] F. Marino, F. Marin, S. Balle, and O. Piro, *Phys. Rev. Lett.* **98** (2007) 074104.

[9] A. M. Zhabotinsky, *CHAOS* **1** (1991) 379.

[10] J. Durham and J. Moehlis, *CHAOS* **18** (2008) 015110.

[11] V. Petrov, S. K. Scott, and K. Showalter, *J. Chem. Phys.* **97** (1992) 6191.

[12] A. Milik, P. Szmolyan, H. Löffelmann, and E. Gröller, *Int. J. Bifurc. Chaos* **8** (1998) 505.

[13] J. L. Hudson, M. Hart, and D. Marinko, *J. Chem. Phys.* **71** (1979) 1602.

[14] M. Schell and F. N. Albahadily, *J. Chem. Phys.* **90** (1989) 822.

[15] G. S. Medvedev and J. E. Cisternas, *Physica D* **194** (2004) 333.

[16] T. Yoshinaga, H. Kawakami, and K. Yoshikawa, *IEICE Trans. Fundam. Electron. Commun. Comput. Sci.* **J71-A** (10) (1988) 1843 (in Japanese).

[17] S. Doi, J. Inoue, and S. Kumagai, *Int. Congress Series* **1301** (2007) 278.

[18] K. Saeki, Y. Sekine, and K. Aihara, *IEICE Trans. Fundam. Electron. Commun. Comput. Sci.* **J83-C** (3) (2000) 213 (in Japanese).

[19] G. S. Medvedev and Y. Yoo, *Physica D* **228** (2) (2007) 87.

[20] G. S. Medvedev and Y. Yoo, *CHAOS* **18** (2008) 033105.

[21] M. Krupa, N. Popovic, and N. Kppell, *SIADS online* **7** (2) (2008) 361.

[22] B. Ermentrout, Simulating, analyzing, and animating dynamical systems: A guide to XPPAUT for researchers and students, (SIAM, Philadelphia), 2002.

[23] H. Kawakami, *IEEE Trans. Circuit. Syst.* **CAS-31** (1984) 246.

[24] A. Wolf, J. B. Swift, H. L. Swinney, and J. A. Vastano, *Physica D* **16** (1985) 285.

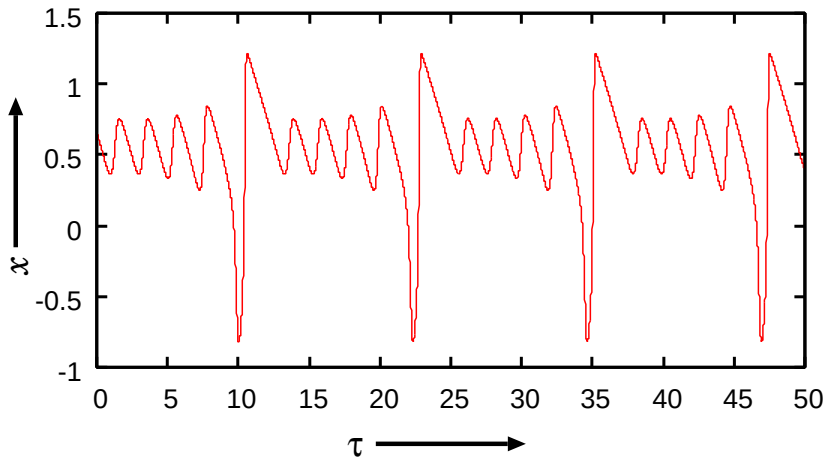

(a)

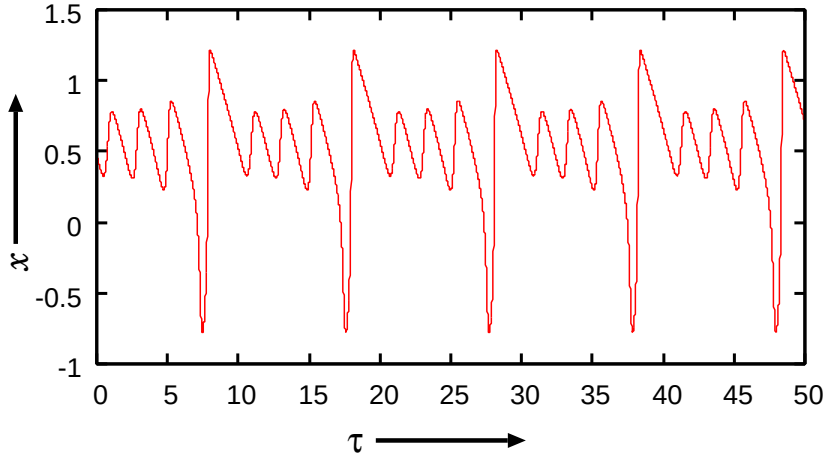

(b)

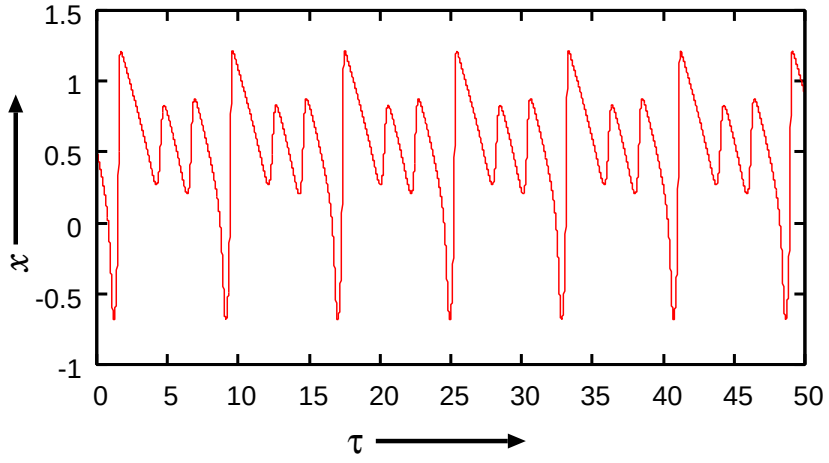

(c)

Fig. 1. Time series of MMOs with $B_0 = 0.49$, $k_1 = 0.35$, and $\varepsilon = 0.1$ in Eq. (2): (a) MMO with one large and four small excursions at $k_3 = 0.29$; (b) MMO with one large and three small excursions at $k_3 = 0.36$; (c) MMO with one large and two small excursions at $k_3 = 0.45$.

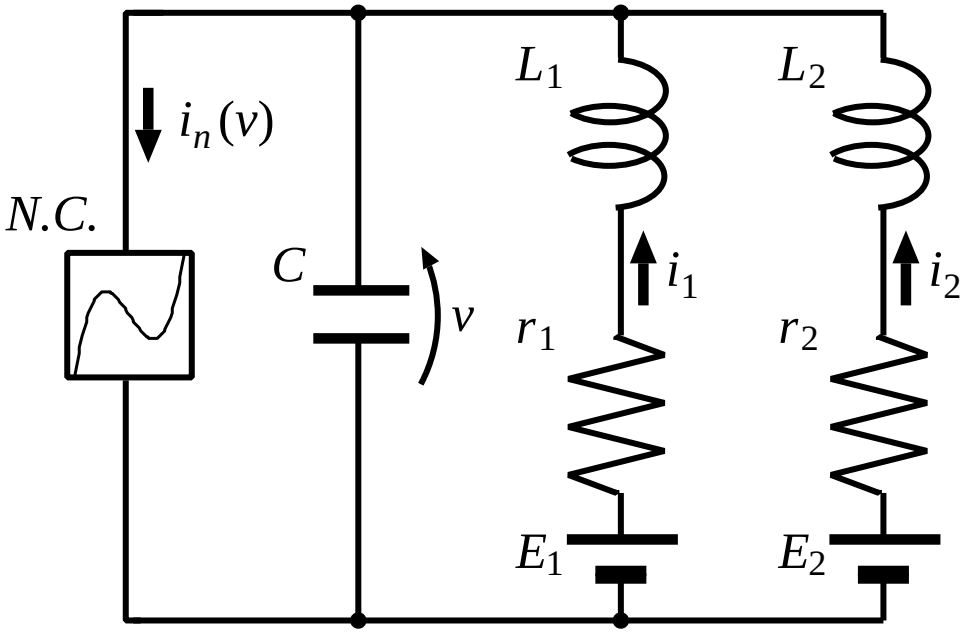

Fig. 2. Circuit diagram.

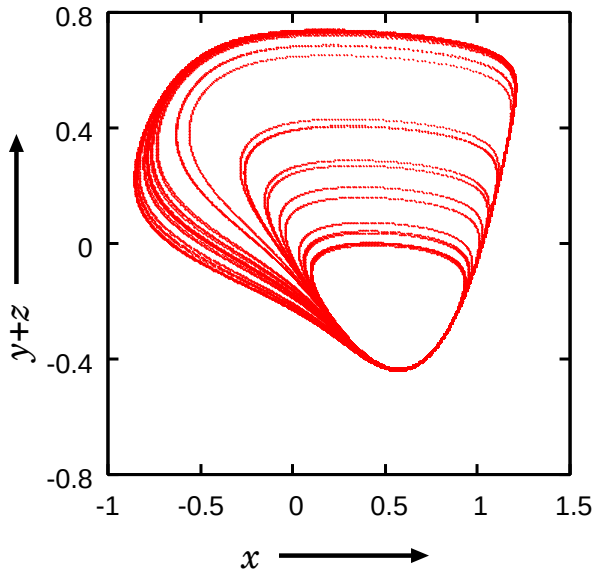

Fig. 3. Chaotic attractor observed in Eq. (1) with $B_0 = 0.11547$, $B_1 = 0.74767$, $\varepsilon = 0.13333$, $k_1 = 0.5$, $k_2 = 0.5$, and $k_3 = 0.25$.

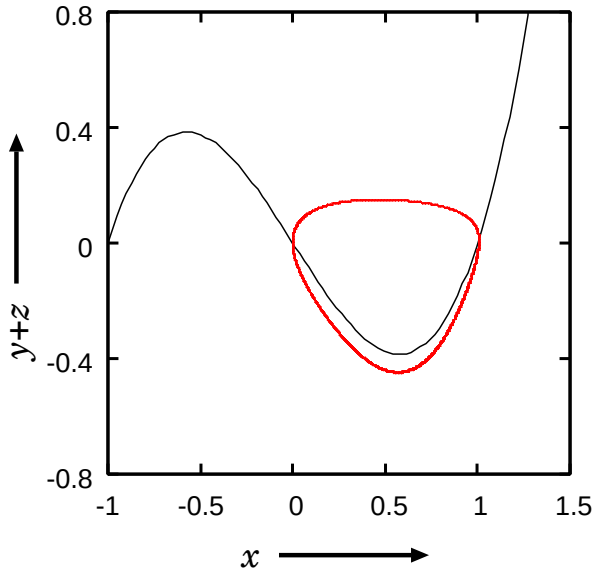

(a)

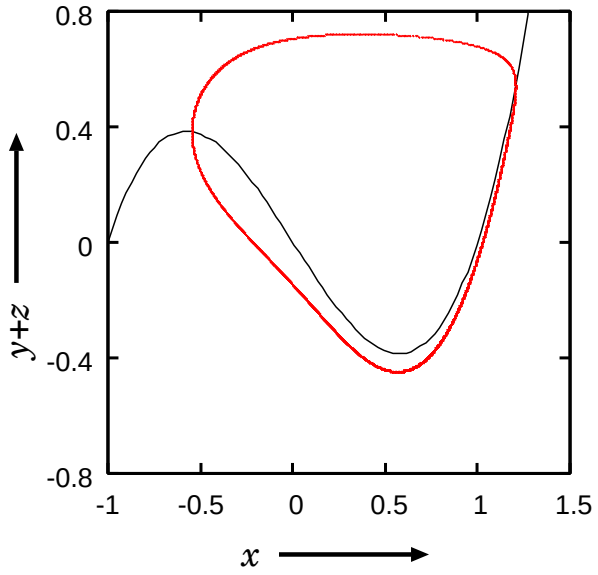

(b)

Fig. 4. Canards observed in the BVP equation: (a) Small-amplitude canard with $B_0 = 0.488$, $k_1 = 0.35$, $k_3 = 1.0$, and $\varepsilon = 0.1$ in Eq. (2); (b) Canard with $B_0 = 0.486$, $k_1 = 0.35$, $k_3 = 1.0$, and $\varepsilon = 0.1$ in Eq. (2).

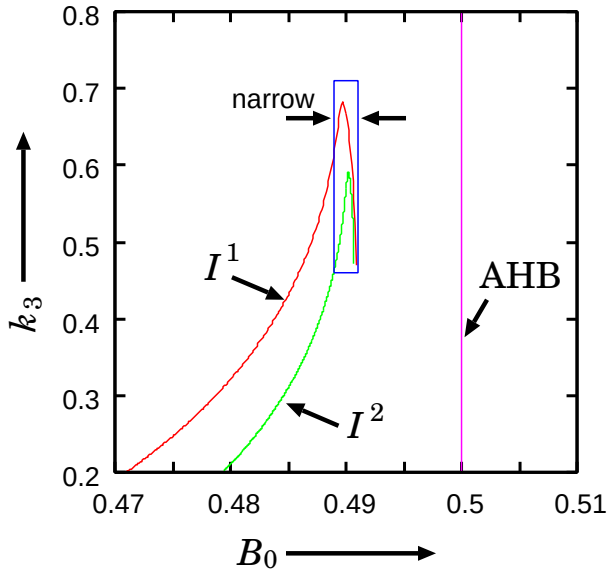

Fig. 5. Bifurcation diagram with $\varepsilon = 0.1$ and $k_1 = 0.35$.

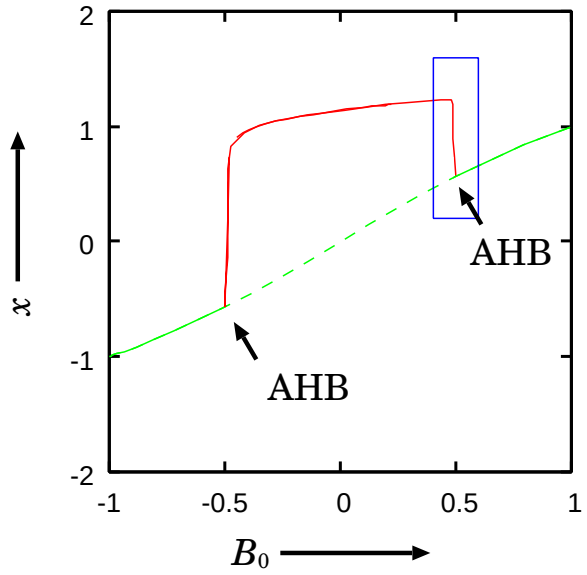

(a)

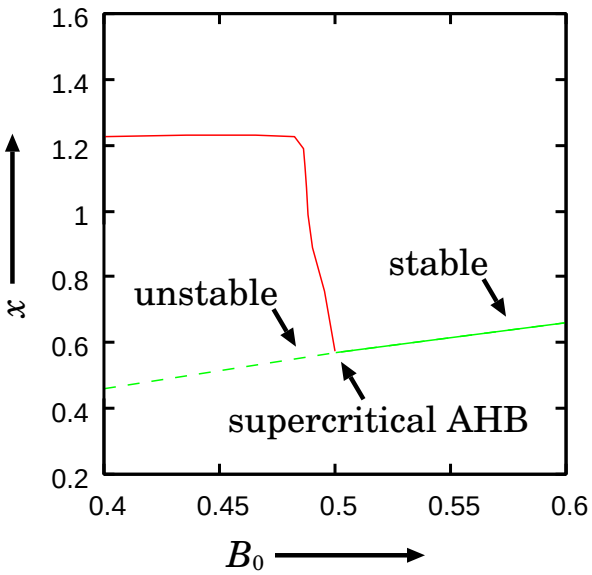

(b)

Fig. 6. One-parameter bifurcation diagram with $\varepsilon = 0.1$, $k_1 = 0.35$, and $k_3 = 1.0$: (a) Global picture of supercritical AHB; (b) Magnified picture around the supercritical AHB on the right.

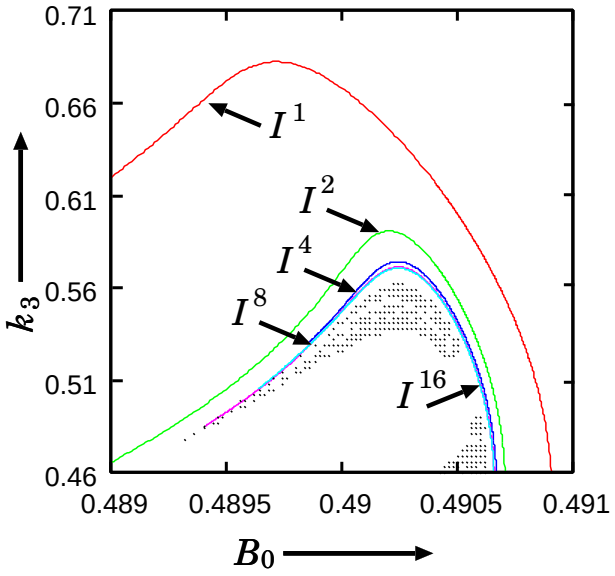

Fig. 7. Magnified picture of bifurcation diagram of Fig. 5 with $\varepsilon = 0.1$ and $k_1 = 0.35$.

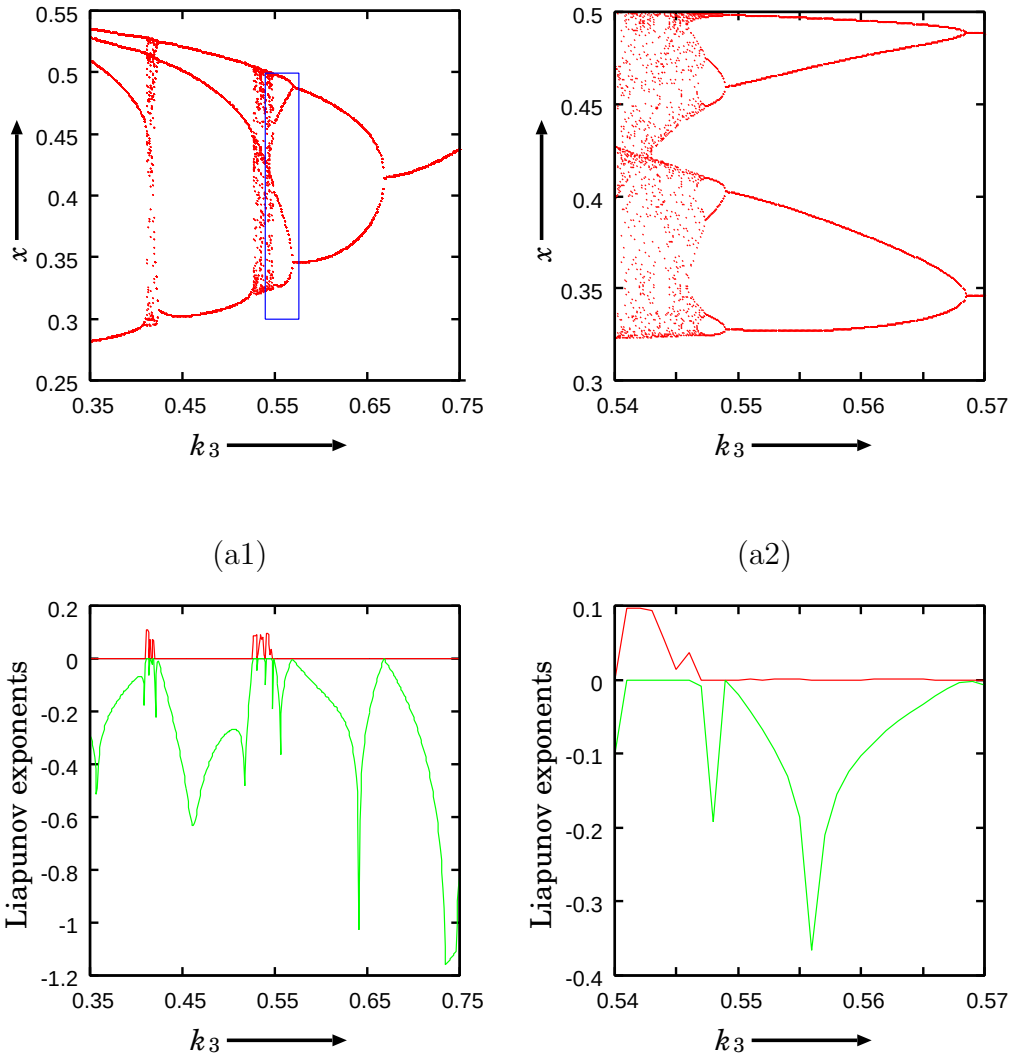

Fig. 8. (a) One-parameter bifurcation diagram with a magnified version and (b) the corresponding graph of Liapunov exponents with $B_0 = 0.49$ and $k_1 = 0.35$.

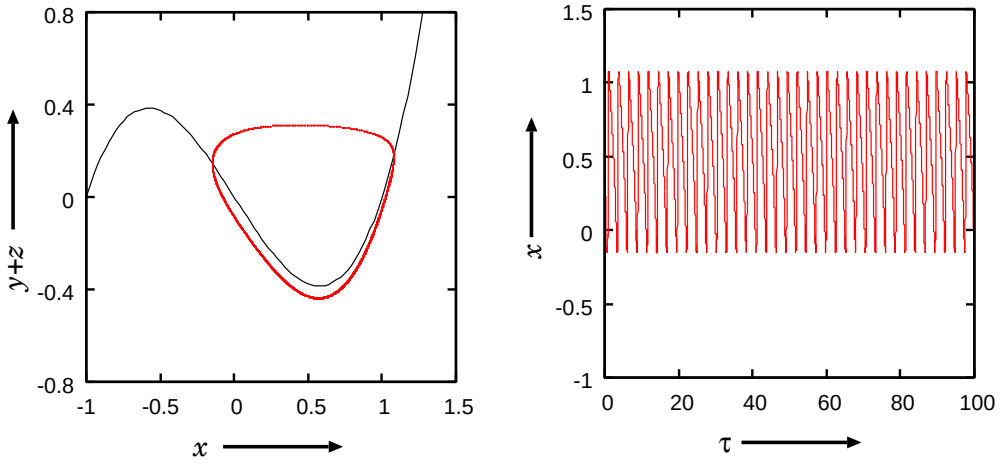

(a)

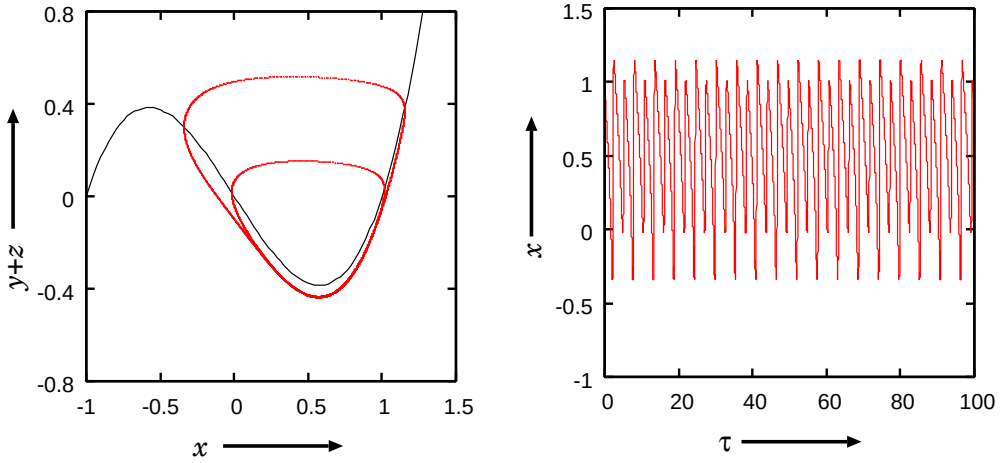

(b)

Fig. 9. Period-doubling cascades of canard with $B_0 = 0.49$ and $k_1 = 0.35$ in Eq. (2): (a) Periodic attractor of period 1 with $k_3 = 0.7$; (b) Periodic attractor of period 2 with $k_3 = 0.65$; (c) Periodic attractor of period 4 with $k_3 = 0.55$; (d) Periodic attractor of period 8 with $k_3 = 0.548$.

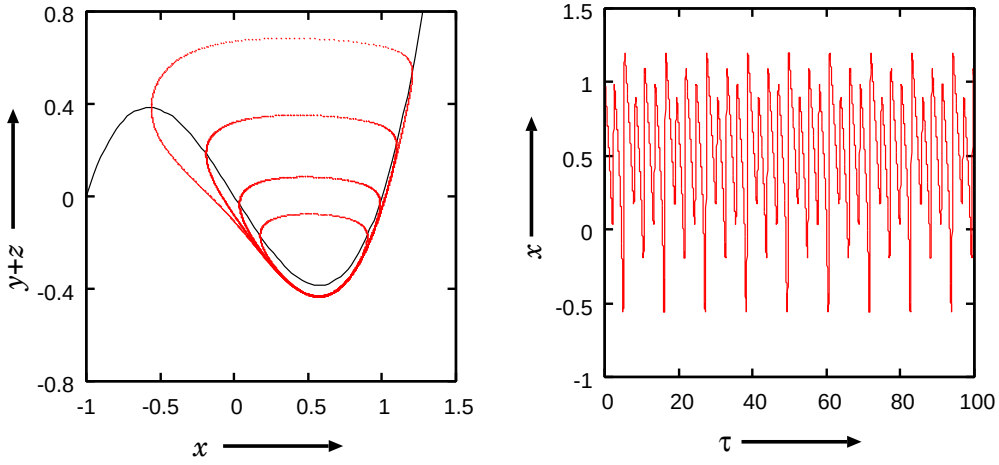

(c)

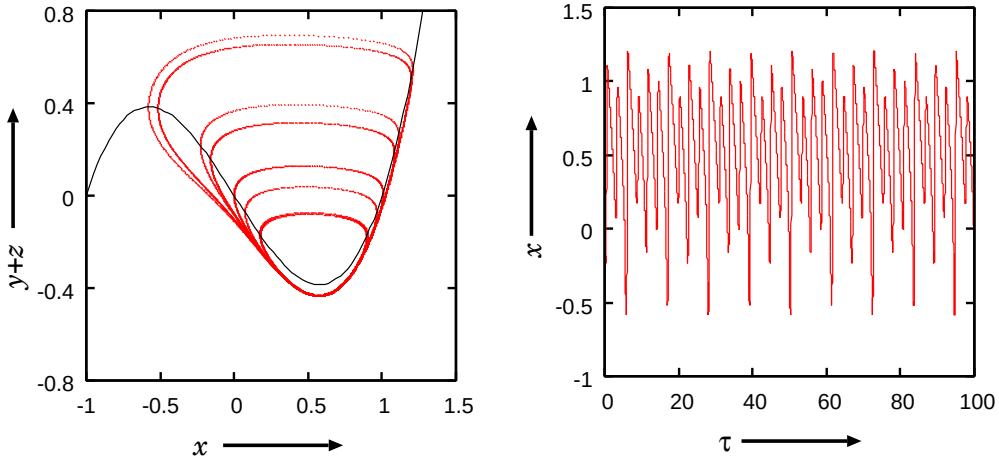

(d)

Fig. 9: Period-doubling cascades of canard with $B_0 = 0.49$ and $k_1 = 0.35$ in Eq. (2): (a) Periodic attractor of period 1 with $k_3 = 0.7$; (b) Periodic attractor of period 2 with $k_3 = 0.65$; (c) Periodic attractor of period 4 with $k_3 = 0.55$; (d) Periodic attractor of period 8 with $k_3 = 0.548$.

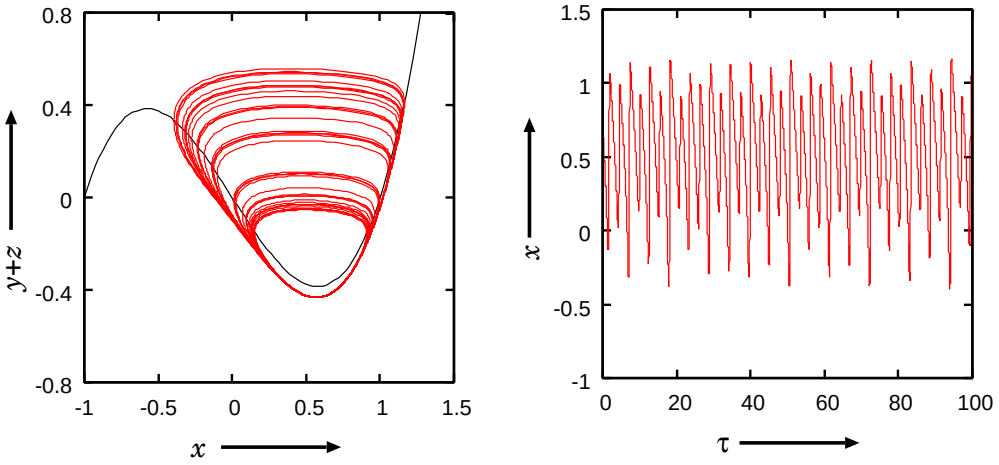

(a)

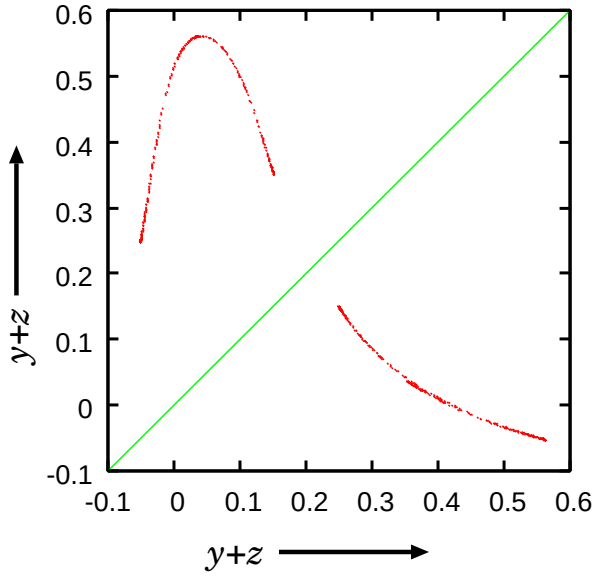

(b)

Fig. 10. (a) Chaotic attractor and (b) first return map with $B_0 = 0.4903$ and $k_1 = 0.35$, and $k_3 = 0.5619$.

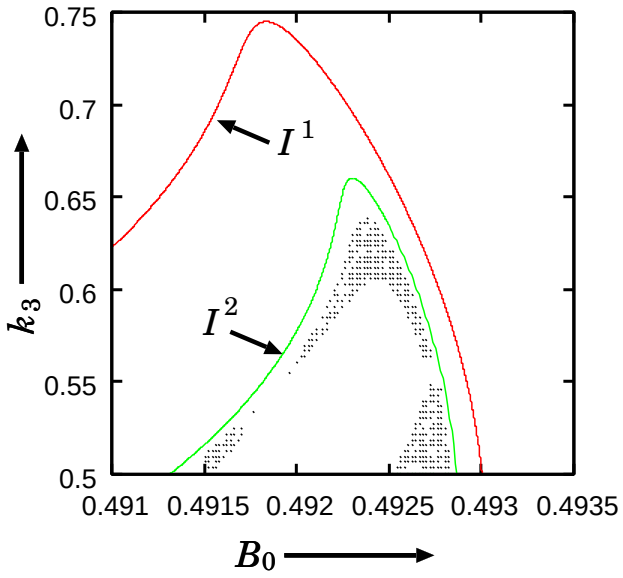

Fig. 11. Bifurcation diagram with $\varepsilon = 0.09$ and $k_1 = 0.35$.